

Microstructural changes in polyethylene–polypropylene blends as revealed by microhardness

J. MARTINEZ SALAZAR, J. M. GARCIA TIJERO*, F. J. BALTÁ CALLEJA
Instituto de Estructura de la Materia, CSIC, Serrano 119, 28006 Madrid, Spain

Microhardness is used to examine the microstructural changes of a series of polyethylene (PE)/polypropylene (PP) blends in a wide composition range. This study complements previous hardness results obtained on high-density/low-density polyethylene systems. The use of isotactic polypropylene, as a blend component allows investigation of a material in which the hardness of the amorphous phase, contrary to PE, differs from zero. The influence of treatments such as crystallization of the PP-phase in the presence of molten PE, within the blend, or annealing the PE phase, while leaving the PP component unmodified, are discussed with reference to the additivity hardness values of the single components H_{PE} and H_{PP} . It is shown that the coexistence of the PP and PE phases inhibits the crystallization capability of one phase and modifies the annealing behaviour of the other phase leading, as a result, to depressed H_{PP} and H_{PE} values. The observed deviations of H_{blend} , throughout the composition range, from the additivity law of single components are quantitatively justified in the light of crystallinity changes of the PP phase and in terms of the population of modified lamellae of the PE component.

1. Introduction

Indentation hardness testing is finding an increased use in the study of the surface mechanical behaviour of semicrystalline polymers [1–4]. The particular attraction of this technique lies in its simplicity and in the fact that it provides valuable information on the polymer microstructure [1]. Semicrystalline polymers show a distinct morphology of crystalline lamellae intercalated by so-called amorphous less-ordered regions. The microhardness, H , of such a lamellar polymer material has been shown to depend, in the case of PE, both on crystal thickness, l , and crystallinity, α [5, 6]. Such a dependence can be defined by [7]

$$H = \alpha H_0 / [1 + (b_1/l)] \quad (1)$$

where H_0 is the hardness of an infinitely thick crystal and b_1 is a parameter. If both, α and l remain constant, H is a function of the cohesive energy of the crystals [8]. In a preceding study [9] it was shown that hardness of high-density and low-density polyethylene blends could be described in terms of an additive model system

$$H_{blend} = H_1 w + H_2 (1 - w) \quad (2)$$

where H_1 and H_2 correspond to the hardness values of the single components and w is the weight fraction of component 1.

The above investigations were concerned with hardness studies on linear and branched PE, where the main structural parameter was the lamellar thickness,

l . The hardness of the interlamellar region, at room temperature, for PE was found to be practically negligible, $H_{PE}^a \sim 0$, as it was always measured above its glass transition temperature (T_g) [10]. From this point of view the use of isotactic polypropylene (PP) as a second component in a blend, offers the possibility of examining the hardness of a material having a T_g value just below room temperature. In this case, one may expect that the hardness of the non-crystalline component, H_{PP}^a , will not be negligible. In addition, polypropylene, in contrast to polyethylene, can be crystallized in a wide spectrum of crystallinities, ranging from highly amorphous material (“smectic phase”) up to $\sim 70\%$.

The aim of the present investigation is to undertake a study of PE/PP blends with reference to the microhardness additivity of the two components, in the light of the microstructural changes occurring. In fact, one may anticipate certain changes to happen because the presence of molten PE within the blend notably affects the crystallization behaviour of the PP phase [11–14]. It has been reported that the coexistence of these phases within the blends takes place at intraspherulitic level [11], i.e. at a much lower scale than that corresponding to the indentation dimensions.

2. Experimental details

2.1. Materials

Blends of isotactic PP (Stamylap) and HDPE (Hostalen GC-6465) were prepared in the molten state at 220°C using a plastograph. The mixtures were subsequently

* Present address: Universidad Autonoma de Madrid, Cantoblanco, 28044 Madrid, Spain.

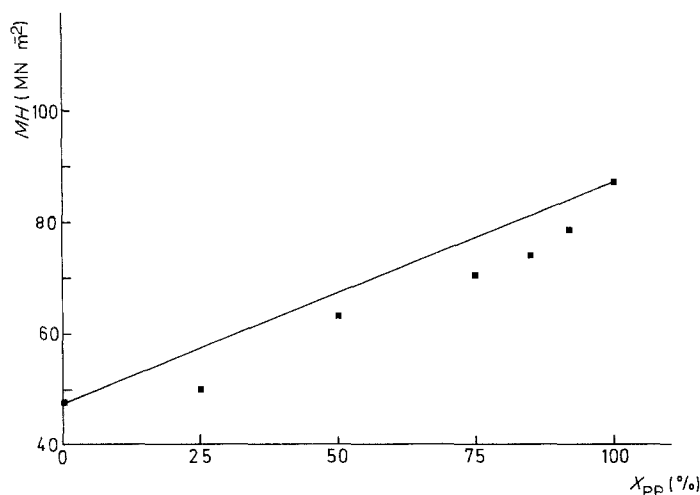


Figure 1 Microhardness of isothermally crystallized blends of HDPE and PP (series A) (see text) as a function of increasing weight concentration of the latter component. (—) Additivity predictions according to Equation 3.

compression-moulded at 150 bar and then rapidly cooled at 15°C. The PE/PP compositions investigated were 0, 25, 50, 75, 85, 92 and 100% PP. In order to enhance the microhardness of one of the phases through the range of compositions, two preparation modes were adopted:

(a) crystallization of the PP phase at 138°C in the presence of molten PE;

(b) annealing of PE the phase at 129°C well below the melting temperature of the PP phase.

The first series of blends was, accordingly, held at $T_1 = 138^\circ\text{C}$ for 6 h. Then the samples were cooled at $T_2 = 130^\circ\text{C}$, left at this temperature for 1 h and finally quenched at 0°C. It is expected that the PP phase will crystallize within the $T_1 < T < T_2$ range (set A). A second set of blends was prepared by annealing the compression-moulded material at 129°C for 24 h. The PP phase remains nearly unaltered at this annealing temperature (set B) [15].

2.2. Techniques

Differential scanning calorimetry of the samples was performed using a Mettler calorimeter. A heating rate of $10^\circ\text{C min}^{-1}$ was used. Crystallinity of each phase within these blends was derived from the ratio of the measured heat of fusion for each sample to the corresponding heat of fusion for infinite crystals ΔH^0 , ($\Delta H_{PE}^0 = 293 \text{ J g}^{-1}$, $\Delta H_{PP}^0 = 165 \text{ J g}^{-1}$). Surface hardness was measured at $\sim 20^\circ\text{C}$ using a Leitz microhardness tester adapted with a Vickers square pyramidal diamond. The microhardness value was calculated from the projected area of the residual indentation: $H = K(P/d^2)$ (MN m^{-2}), where d is the mean diagonal length of the impression (mm), P is the

contact load applied (N), and K is a geometrical constant equal to $K = 1.854$. Loads of 0.25 and 0.5 N were used. The loading cycle was 0.1 min. The accuracy of a determination of H , for each sample, from a series of about ten indentations, lies within 1 to 2%.

3. Results and discussion

The obtained H values for the PP and PE starting compression-moulded materials quenched at 15°C are, respectively, $H_{PP} = 70.5 \text{ MN m}^{-2}$ and $H_{PE} = 60 \text{ MN m}^{-2}$, i.e. the H values for the single components do not differ sensibly from each other. Microhardness of the blends for series A, H_A , and crystallinity values of the PP phase, α , within each blend are collected as a function of per cent composition in Table I. Note that for series A now $H_{PP} \gg H_{PE}$. The microhardness for series B, H_B , and volume fraction of annealed PE material, as derived from DSC scans are given in Table II. For this series of blends, $H_{PP} \ll H_{PE}$. Fig. 1 illustrates the gradual increase of microhardness as a function of PP-per cent concentration, X_{PP} for series A. Here an apparent deviation from the additivity law (solid line) defined by:

$$H_{\text{blend}} = X_{PP}H_{PP} + X_{PE}H_{PE} \quad (3)$$

is obtained, where X_{PP} and X_{PE} are, respectively, the weight fractions of each material. Fig. 2 illustrates, on the other hand, the microhardness decrease with increasing PP concentration for series B. Here again a conspicuous deviation of data with respect to the additivity law is clearly seen. In what follows we will attempt to explain the experimental hardness deviations from the additivity predictions (Equation 3) in the light of changing structural details reciprocally

TABLE I Experimentally determined and calculated hardness values (using Equations 3 and 4) and crystallinity of the PP component for the series of PE/PP blends A as a function of weight per cent PP

X_{PP} (%)	H_B (experimental)	H_B (calculated)	α (%)
0	48	—	—
25	50	48	36
50	63	65	52
75	71	72	55
85	74	76	55
92	79	81	58
100	87	87	68

TABLE II Experimental and calculated hardness values (using Equations 2 and 3) and weight fraction of thicker PE lamellae for the series of blends B as a function of weight per cent PP

X_{PP} (%)	H_B (experimental)	H_B (calculated)	$(1 - w)$ (%)
0	86	86	71
25	81	79	59
50	74	74	47
75	69	71	37
85	69	70	16
90	71	70	5
95	71	70	0
100	70.5	—	—

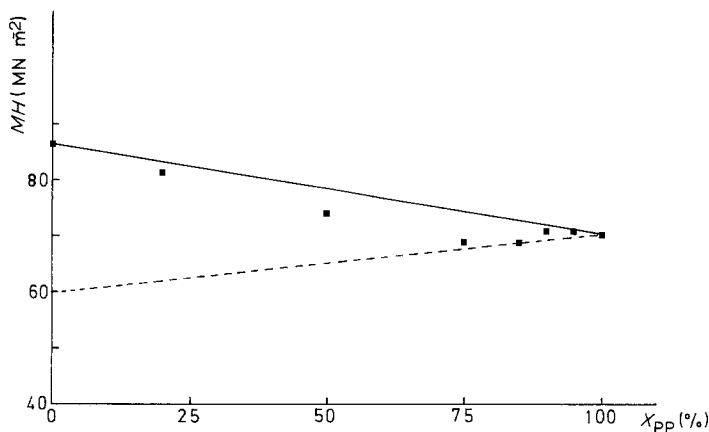


Figure 2 Microhardness of blends of HDPE and PP annealed at $T_A = 129^\circ\text{C}$ for 24 h (series B) as a function of weight concentration of the latter component. Additivity model predictions (Equation 3) (—) before and (---) after annealing.

induced by both phases. For this purpose we will discuss the results according to the two preparation modes employed.

3.1. Isothermal crystallization of the PP phase

For the series of blends A, during crystallization of the PP component at 138°C for 6 h, the PE phase remains in the molten state. Consequently, after quenching the blends of this series at 0°C , H_{PE} in Equation 3 stays constant throughout the concentration range. Most revealing is, however, the crystallinity decrease for the PP-component within the series with increasing HDPE concentration, as shown in Table I. This is, in fact, a relevant result supporting the concept that PE, within these blends, inhibits the crystallization process of PP [12]. A detailed description of this phenomenon will be the object of a forthcoming paper [16]. As a result, the microhardness of the PP phase is no longer constant but it varies with crystallinity, α , according to

$$H_{PP} = \alpha H_{PP}^C + (1 - \alpha)H_{PP}^a \quad (4)$$

where H_{PP}^C , and H_{PP}^a are, respectively, the hardness values for the crystalline and amorphous phases. In order to obtain the limiting values, H_{PP}^C and H_{PP}^a , pure

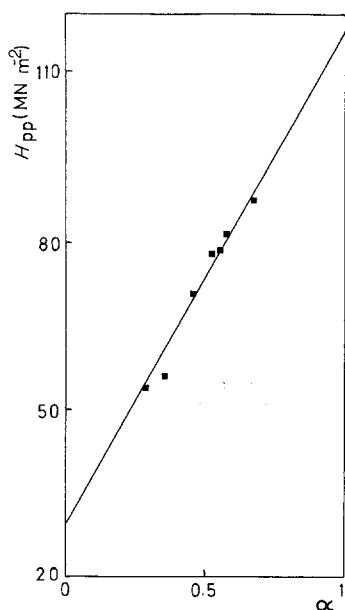


Figure 3 Microhardness of melt-crystallized PP as a function of weight per cent crystallinity.

PP samples were crystallized within a wide range of crystallinities. Fig. 3 shows the linear plot of H_{PP} against α according to Equation 4. This result characterizes the intrinsic additivity behaviour of both crystalline and amorphous phases within PP. Through extrapolation of H_{PP} to $\alpha = 0$ and $\alpha = 1$ one obtains straightforwardly the values of $H_{PP}^a = 30\text{ MN m}^{-2}$ and $H_{PP}^C = 116\text{ MN m}^{-2}$, respectively. The knowledge of these quantities allows the immediate determination of H_{PP} for a given α . It is convenient to recall that such a linear plot of H against α has not been obtained previously for PE because H_{PE} is, itself, also a function of crystal thickness (see Equation 1). Now by substituting the H_{PP} data derived from Equation 4 for each α value into Equation 3 one obtains the calculated H_{blend} values (Table I) which justify, within the error of experiment, the depression of data from the solid line in Fig. 1. In other words, the agreement obtained between experimental and calculated data in Table I confirms that the hardness of the series A of PE/PP blends investigated can be explained in terms of the additivity law defined by Equation 3.

3.2. Annealing of the PE phase

For series B, annealing of the compression-moulded blends at 129°C does not affect the crystallinity of the PP component ($X_{PP} = 100\%$ in Fig. 2), evidence of which is the constancy of the H_{PP} value for the single PP component. Annealing of compression-moulded PE at 129°C induces, however, a hardening of the single PE component from 60 MN m^{-2} up to 87 MN m^{-2} (see Fig. 2). It is evident that the enhancement of microhardness throughout the B series is now obtained through the hardening of the PE phase. Differential scanning calorimetry carried out on these blends shows, indeed, that a fraction of PE material is transformed into thicker crystals with a higher melting temperature (Table II). In a previous paper [17] we interpreted the hardening of PE after annealing in terms of a parallel crystal thickness increase. Fig. 4 illustrates the hardness increase of lamellar PE in region II after annealing at different temperatures as a function of both crystal thickness and crystallinity. The straight lines represent the hardness predictions according to Equation 1. One clearly sees that the hardening of the annealed PE material is mainly due to a crystal thickening whereas crystallinity plays only a minor part. For instance, an increase of crystallinity

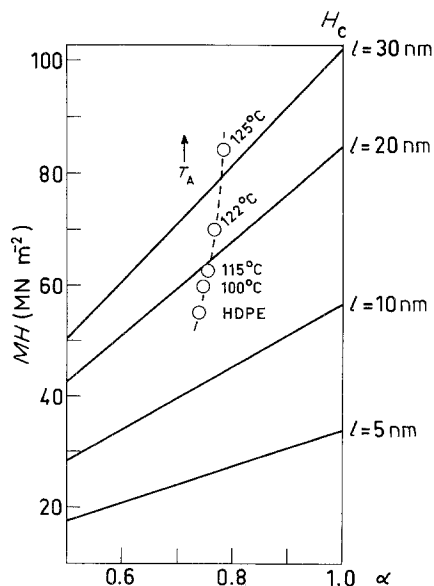


Figure 4 Plot of microhardness as a function of crystallinity for PE, according to Equation 1, using crystal thickness, l , as a parameter (—). The data correspond to HDPE annealed at various temperatures [17].

of 5% in Fig. 4 would just induce a rise in MH of 5% whereas the experimentally observed increase is $\sim 60\%$. This hardening can only be explained by a lamellar thickening contribution, as pointed out in an earlier study [17]. The presence of the two DSC peaks in the series of blends B ($T_A \sim 129^\circ\text{C}$) (Fig. 5) suggests, in fact, the coexistence of two types of lamella: the low-temperature peak is attributed to melting and recrystallization of a fraction of thinner lamellae and the high-temperature peak is due to a thickening of the initial lamellae. Thus, the microhardness, for the PE phase within the blend can be described, by means of Equation 2 in terms of a "composite" having two populations of PE crystals contributing to two distinct melting peaks. Now, H_1 , in Equation 2 is the microhardness of the thinner lamellae and w is the weight fraction of these lamellae, as derived from the area of the corresponding DSC peak. On the other hand, H_2 , is the corresponding hardness of the thicker lamellae having a weight fraction $(1 - w)$. Fig. 5 illustrates the DSC peaks for the pure PE sample and for the PE/PP blend containing 75% PE.

We should finally note that the presence of PP material in series B sensibly modifies the annealing behaviour of the PE crystals. Table II shows, indeed, that the fraction of annealed material $(1 - w)$ contributing to H_2 notably decreases with increasing content of PP component. Further studies involving different PE types might throw light on this unexpected behaviour. The values of H_1 and H_2 for the two PE lamellar populations, derived from the pure annealed PE sample, turn out to be $H_1 = 60\text{ MN m}^{-2}$ and $H_2 = 97\text{ MN m}^{-2}$, respectively. Consequently, as w can be deduced from the area of the DSC peak, we can now calculate the value of H_{PE} from Equation 2 that would correspond to the PE phase in each blend. By substituting these data into Equation 3 one obtains the calculated values for H_{blend} . Table II shows the

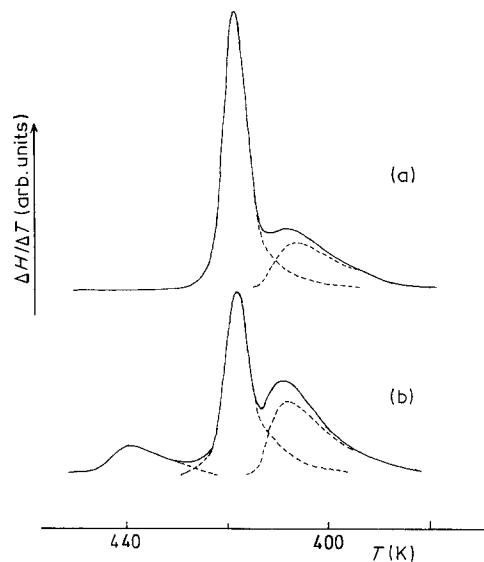


Figure 5 Specific heat for HDPE and for the blend of HDPE/PP containing 75% HDPE annealed at 129°C for 24 h as a function of temperature.

excellent fit obtained between calculated and experimental hardness data. The above calculation, hence permits one to explain satisfactorily the deviation of all H_B data from the additivity law shown in Fig. 2.

4. Conclusions

In summary, the hardness of polyethylene/polypropylene blends can be described in terms of a parallel additive system of two independent components H_{PE} and H_{PP} . However, treatments such as (a) crystallization of the PP-phase in the presence of molten PE within the blends, and (b) annealing of the PE phase, leaving the PP component unaltered, induce deviations from the hardness additive behaviour of the independent components. The presence of PE throughout the range of blends inhibits the crystallization of PP, inducing a depression of crystallinity which causes, in turn, a depression of the expected hardness-value from the additivity law. Conversely, the presence of PP within the blends substantially modifies the annealing behaviour of the PE crystals (fraction of initial lamellae annealed) inducing a similar depression from the H additivity values. Finally, the linear correlation found between hardness and crystallinity for the isolated PP material opens-up the possibility of applying this simple technique as a new optional method for the calculation of crystallinity in polymers.

References

1. F. J. BALTÁ CALLEJA, *Adv. Polym. Sci.* **66** (1985) 117.
2. F. J. BALTÁ CALLEJA, D. R. RUEDA, J. GARCIA, F. P. WOLF and V. H. KARL, *J. Mater. Sci.* **21** (1986) 1139.
3. F. ANIA, H. G. KILIAN and F. J. BALTÁ CALLEJA, *J. Mater. Sci. Lett.* **5** (1986) 1183.
4. M. E. CAGIAO, D. R. RUEDA and F. J. BALTÁ CALLEJA, *Colloid Polym. Sci.* **265** (1987) 37.
5. F. J. BALTÁ CALLEJA, J. MARTINEZ SALAZAR, H. CACKOVIC and J. LOBODA-CACKOVIC, *J. Mater. Sci.* **16** (1981) 739.
6. J. MARTINEZ SALAZAR, F. J. BALTÁ CALLEJA, *ibid.* **18** (1983) 1077.

7. F. J. BALTÁ CALLEJA, H. G. KILIAN, *Colloid Polym. Sci.* **263** (1985) 697.
8. J. MARTINEZ SALAZAR, J. GARCIA and F. J. BALTÁ CALLEJA, *Polym. Commun.* **26** (1985) 57.
9. J. MARTINEZ SALAZAR and F. J. BALTÁ CALLEJA, *J. Mater. Sci. Lett.* **4** (1985) 324.
10. R. F. BOYER, *J. Macromol. Sci. Phys.* **B8** (1973) 503.
11. J. MARTINEZ SALAZAR, E. LÓPEZ CABARCOS and F. J. BALTÁ CALLEJA, 17th Europhys. Conference on Macromolecular Physics, P-23, Prague (1985).
12. Z. BARTCZAK, A. GALESKI and M. PRACELLA, *Polymer* **27** (1986) 537.
13. A. J. LOVINGER and M. L. WILLIAMS, *J. Appl. Polym. Sci.* **25** (1980) 1703.
14. J. W. TEH, *ibid.* **28** (1983) 605.
15. F. J. BALTÁ CALLEJA and A. PETERLIN, *Makromol. Chem.* **141** (1971) 91.
16. J. MARTINEZ SALAZAR and F. J. BALTÁ CALLEJA, unpublished results.
17. D. R. RUEDA, J. MARTINEZ SALAZAR and F. J. BALTÁ CALLEJA, *J. Mater. Sci.* **20** (1985) 834.

*Received 19 March
and accepted 3 June 1987*